This work was supported in part by the Air Force Office of Scientific Research. One of the authors (Yoshito Tsunoda) gratefully acknowledges the support of Hitachi, Ltd.; he is on leave from their Central Research Laboratory, Kokubunji, Tokyo, Japan.

Corrected galleys not received from authors.

References

1. H. N. Roberts, J. W. Watkins, and R. H. Johnson, Appl. Opt. **13**, 841 (1974).
2. I. C. Chang, IEEE Trans. Son. Ultrason. **SU-23**, 2 (1976).
3. L. J. Cutrona, in *Optical and Electro-Optical Information Processing*, J. T. Tippett, D. A. Berkowitz, L. C. Clapp, C. J. Koester, and A. Vanderburgh, Jr., Eds. (MIT Press, Cambridge, 1965), Chap. 6.
4. P. N. Tamura and J. C. Wyant, in *Optical Information Processing, Proceedings of the SPIE*, Vol. 83, 97 (1976).
5. J. W. Goodman, P. Kellman, and E. W. Hansen, Appl. Opt. **16**, 733 (1977).
6. R. J. Marks, J. F. Walkup, M. O. Hagler, and T. F. Krile, Appl. Opt. **16**, 739 (1977).
7. N. R. Scott, *Electronic Computer Technology* (McGraw-Hill, New York, 1970), p. 209.
8. D. Hoeschele, *Analog-to-Digital/Digital-to-Analog Conversion Techniques* (Wiley, New York, 1968), p. 334.
9. Y. Tsunoda, K. Tatsuno, K. Kakaoka, and Y. Takeda, Appl. Opt. **15**, 1398 (1976).

Coherent optical implementation of 1-D Mellin transforms

Peter Kellman and Joseph W. Goodman

Stanford University, Department of Electrical Engineering, Stanford, California 94305.
Received 20 May 1977.

Recent interest[1] in Mellin power spectra, complex filtering, and correlation is due to the scale invariance of the Mellin transform. Mellin correlation has been cited for application to 2-D target detection and 1-D signal processing where parameters of scale and Doppler are unknown. In such applications, Fourier domain matched filtering requires either sequential hypothesis testing or multichannel processing. Loss of correlation in the Fourier implementation due to scale difference between received signal and reference is exchanged, however, for an equally severe loss in the Mellin correlation due to time or positional displacement. A coherent optical technique for Mellin transforms is described here in which signals may be processed in real time to provide scale invariant correlations. The parameterization on time uncertainty is provided for automatically by utilizing an acoustooptic spatial light modulator.

Methods for performing general linear integral transforms using parallel processing in both spatial dimensions allow real time operation. Several of these methods have been outlined recently[2]; one configuration, well suited for implementing Mellin spectrum analysis, is reviewed here.

The general linear superposition integral may be written as

$$g(y) = \int_{-\infty}^{\infty} f(x)h(x,y)dx \qquad (1)$$

for input $f(x)$ and output $g(y)$. The Mellin transform, with purely imaginary argument,

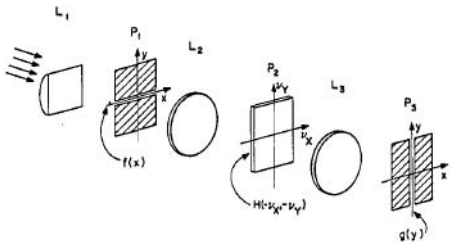

Fig. 1. Optical implementation of 1-D Mellin transform.

$$g(y) = \int_0^{\infty} f(x)x^{i2\pi y-1}dx \qquad (2)$$

is a special case of Eq. (1), where

$$h(x,y) = x^{i2\pi y-1}U(x),$$

$$U(x) = \begin{cases} 1, & x > 0 \\ 1/2, & x = 0 \\ 0, & x < 0 \end{cases}.$$

Equation (1) may be rewritten as:

$$g(y) = \int\int_{-\infty}^{\infty} F(\nu_x)H(-\nu_x,-\nu_y)\exp(-i2\pi\nu_y y)d\nu_x d\nu_y, \qquad (3)$$

where H and F are the Fourier transforms of h and f.

The optical realization of Eq. (3) is shown in Fig. 1. The input function is illuminated by the cylindrical lens L_1. Lens L_2 is spherical and Fourier transforms the input function in both directions. The effect of the vertical transformation of the narrow input slit is simply to spread out the horizontal transform in the vertical direction. In plane P_2 we place a mask with complex amplitude transmittance $H(-\nu_x,-\nu_y)$. Lens L_3 is spherical and again performs a 2-D Fourier transformation. Thus, along a vertical output slit parallel to the y axis (displaced horizontally if H is realized as a carrier-frequency hologram), a simple integration in the ν_x direction and a Fourier transformation in the ν_y direction is achieved as required by Eq. (3).

The mask $H(\nu_x,\nu_y)$ was made optically as a carrier-frequency hologram by the configuration shown in Fig. 2. In this example, the real hologram transmittance is:

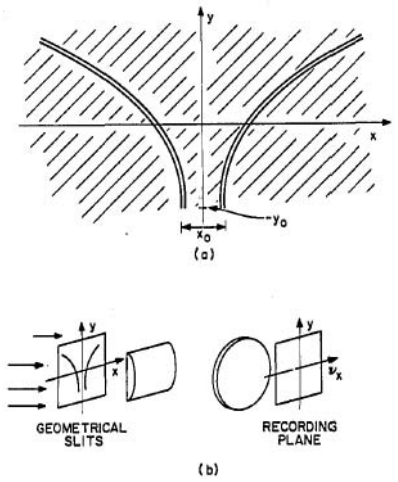

Fig. 2. Recording of the required filter: (a) transparent slits; (b) recording geometry.

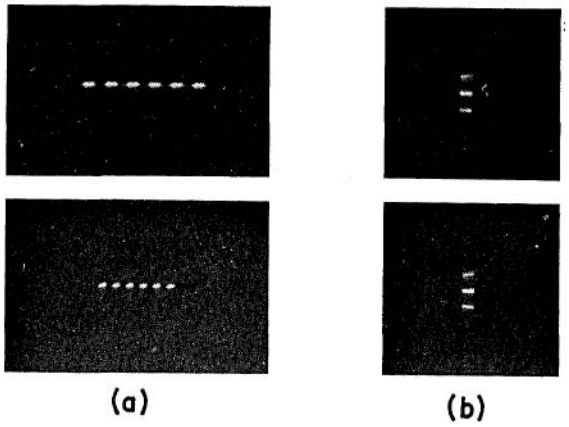

Fig. 3. Experimental demonstration of invariance of Mellin power spectrum to input scale change: (a) inputs; (b) outputs.

$$H(\nu_x,\nu_y) = B + \cos\{2\pi\nu_x[\exp(\nu_y) + X_0/2]\}. \quad (4)$$

The slit separation X_0, shown in Fig. 2, corresponding to the carrier frequency $X_0/2$, must be greater than the extent of $f(x)$ to avoid overlap with the image resulting from hologram bias B. The output plane intensity is given by:

$$g(x,y) = \int\int_{-\infty}^{\infty} F(\nu_x)(B + \cos\{2\pi\nu_x[\exp(\nu_y) + X_0/2]\}) \cdot \exp[-i2\pi(\nu_x x + \nu_y y)]d\nu_x d\nu_y. \quad (5)$$

It can be readily verified that

$$g(X_0/2, -y) = \tfrac{1}{2}\int_0^{\infty} f(x)x^{i2\pi y}dx. \quad (6)$$

Thus the output $g(X_0/2, -y)$ is the Mellin spectrum (with imaginary argument) of $xf(x)$. The spectrum of $f(x)$ can be obtained by use of input window x^{-1}.

Scale invariance of the Mellin power spectrum was demonstrated experimentally. The inputs, shown in Fig. 3(a), were six cycles of a square wave (Ronchi ruling) at two frequencies, f and $2f$. The output power spectra were identical over an octave of input scale change. The outputs are shown in Fig. 3(b). Limitation to octave scale variation was due to higher diffraction orders resulting from hard clipping of the holographic mask. The efficiency of this technique is inversely proportional to the input time–bandwidth product since the output is one-dimensional and the illumination is in both dimensions. This loss, coupled with low holographic and acoustooptic efficiencies, presents a severe limitation.

An important application of the Mellin transform is implementing a scale correlation,[1] $R(\alpha)$, between two signals f_1 and f_2, where

$$R_{f_1f_2}(\alpha) \triangleq \alpha^{1/2}\int f_1(\alpha x)f_2(x)dx. \quad (7)$$

The scale correlation is useful in estimating Doppler between a received signal $f(\beta x)$ and a reference signal $f(x)$. The unknown scale parameter is determined from the position of peak response of the scale correlation, since

$$R_{ff}(\alpha) \le R_{ff}(1).$$

It has been further noted[3] that the scale autocorrelation yields interesting signal features. The use of the Mellin transform in Doppler signal processing has been previously described[4,5] using a 1-D joint transform correlator.

The scale correlation may be realized through matched filtering in the Mellin transform domain in the same manner that translational correlations are implemented by Fourier domain filtering.[1,4,5] The scale correlation is given as the inverse Mellin transform of the product of complex Mellin spectra M_1 and M_2^*. Substituting the inverse Mellin transform by a Fourier transform results in a distorted version $\hat{R}(\alpha)$ of the scale correlation that is easier to realize optically.

$$\hat{R}(y) \triangleq \exp(-y/2)\int f_1(x)f_2[x\exp(-y)]dx \quad (8)$$

$$= \exp(-y/2)\int M_1(y')M_2^*(y')\exp(-i2\pi yy')dy', \quad (9)$$

where

$$M_1(y') = \int_0^{\infty} xf_1(x)x^{i2\pi y'-1}dx$$

$$M_2(y') = \int_0^{\infty} f_2(x)x^{i2\pi y'-1}dx.$$

An optical implementation of Eq. (9) is shown in Fig. 4. The input signal is f_1, and the reference signal is f_2. The matched filter complex transmittance M_2^* may be realized as a carrier frequency hologram.

By using a sliding input signal $f_1(vt - x)$ (acoustooptic modulation), the output

$$\hat{R}(y,t) = \exp(-y/2)\int f_1[(vt - x)]f_2[x\exp(-y)]dx$$

generates a cross ambiguity function in time. Thus, in a radar application, an array of output detectors becomes a Doppler filter bank; the time of peak correlation or threshold crossing gives the delay, and the position of maximum response corresponds to Doppler. Extension to the multichannel Mellin correlator is straightforward, requiring an additional spherical–cylindrical pair.

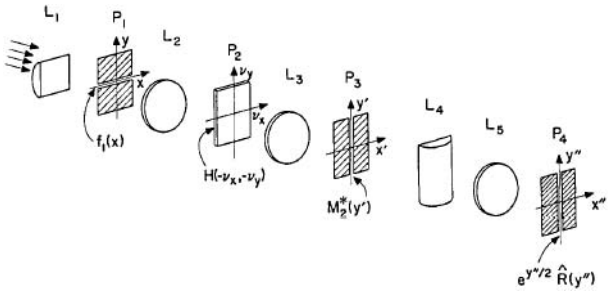

Fig. 4. Optical system for performing the scale correlation defined by Eq. (8).

Corrected galleys not received from authors.

This work was supported by the National Science Foundation.

References

1. D. Casasent and D. Psaltis, Proc. IEEE **65**, 77 (1977).
2. J. W. Goodman, P. Kellman, and E. Hansen, Appl. Opt. **16**, 733 (1977)
3. V. L. Corbin, H. E. Moses, and A. F. Quesada, J. Geophys. Res. **78**, 6199 (1973).
4. D. Casasent and D. Psaltis, Appl. Opt. **15**, 2015 (1976).
5. D. Casasent and M. Kraus, Opt. Commun. **19**, 212 (1976).